Two Bayesian Image Restoration Algorithms From Partially-Known Blurs

Nikolas P. Galatsanos
Dept. of Electrical and Computer Eng.
Illinois Inst. of Techn
Chicago, IL 61616

Vladimir Z. Mesarovic
Crystal Semiconductor Corp.
4210 S. Industrial Drive
Austin, TX 78744

Rafael Molina
Dept. de Ciencias de la Computation
Universidad de Granada
18701 Granada, Spain

Abstract

In this paper we examine the restoration problem when the point-spread function (PSF) of the degradation system is partially known. For this problem the PSF is assumed to be the sum of a known deterministic and an unknown random component. This problem has been examined before; however, in most previous works the problem of estimating the parameters that define the restoration filters was not addressed. In this paper two iterative algorithms that simultaneously restore the image and estimate the parameters of the restoration filter are proposed using evidence analysis (EA) within the hierarchical Bayesian framework. Numerical experiments are presented that test and compare the proposed algorithms.

1 Introduction

In many image restoration applications, the point-spread function (PSF) is neither unknown to warrant use of blind deconvolution nor perfectly known as many classical methods assume. For instance, in medical imaging techniques such as positron emission tomography (PET) and single-photon emission computed tomography (SPECT), the PSF is difficult to specify completely, in part because it is object-dependent, owing to scattering and photon attenuation. In astronomy, atmospheric turbulence yields a random time-varying PSF which is not known exactly when the image is restored.

Random blurs have been considered before. A linear minimum mean square error filter (LMMSE) is developed in [6]. In [6] an "ad-hoc" iterative algorithm for covariance estimation is proposed. The convergence properties of this algorithm, however, were not analyzed in [6]. In [2] fast regularized constrained total least squares (RCTLS) filters were derived and implemented in the discrete Fourier transform (DFT) domain. It was shown in [2] that the RCTLS filters were superior to the regularized-least-squares (RLS) filters that do not take into account the errors in the PSF and also to the linear minimum mean square error (LMMSE) filter [6] for this problem. However, to effectively utilize the RCTLS filter in [2], the noise and the image prior parameters must be known prior to restoration. In [3, 4] an iterative algorithm for simultaneous parameter estimation and image restoration based on the Expectation Maximization (EM) algorithm was proposed.

In this paper we apply Evidence Analysis (EA), within the hierarchical Bayesian framework [1, 5], to the partially-known blur restoration problem. Using two models for the conditional convariance of the observed data based on the source signal EA yields two iterative restoration algorithms that simultaneously estimate the required filter parameters. The first of these algorithms produces a restoration step identical to the RCTLS filter, thus in effect it solves the parameter estimation problem for the RCTLS filter. The second of these algorithms turns out to be identical to the EM algorithm in [3, 4], thus in effect we provide an alternative framework to derive the EM algorithm.

2 Components of the Hierarchical Model

Let us now examine the components of the hierarchical model used for the partially known blur restoration problem, that is, the image model, the observation model, and the model for the unknown hyperparameters.

2.1 Image Priors

A commonly used model for the image prior is based on the the simultaneously autoregressive (SAR) image models have been proposed, see for example [5]. These models can be described by the following conditional PDF:

$$P(\mathbf{f}|\alpha) = \text{const} \cdot \alpha^{(\frac{N}{2})} \exp\left\{-\frac{\alpha}{2}||\mathbf{Q}\mathbf{f}||^2\right\}, \quad (1)$$

where α is positive unknown parameter that controls the smoothness of the image and $||\mathbf{Q}\mathbf{f}||^2$ captures the

0-8186-8821-1/98 $10.00 © 1998 IEEE

image autoregressive model. It is easy to see that the PDF in (1) is equivalent to a zero-mean multidimensional Gaussian $N(0, \mathbf{R}_f)$, when $\mathbf{R}_f^{-1} = \alpha \mathbf{Q}^t \mathbf{Q}$. For simplicity, but without loss of generality, we shall use a circulant Laplacian high-pass operator for $\mathbf{Q}$ throughout the rest of this paper [2].

In [6] the space-invariant PSF was represented as the sum of a deterministic component and a stochastic component of zero-mean, i.e.,

$$\mathbf{h} = \bar{\mathbf{h}} + \Delta\mathbf{h}, \tag{2}$$

where $\bar{\mathbf{h}} \in \mathcal{R}^N$ and $\Delta\mathbf{h} \in \mathcal{R}^N$ are the deterministic (known) and the random (unknown error) components of the PSF, respectively. This is a very general model that attempts to incorporate the random (unknown error) component of the PSF in the restoration algorithm. The unknown component of the PSF is modeled as stationary zero-mean white noise with $N \times N$ covariance matrix $\mathbf{R}_{\Delta h} = \frac{1}{\beta}\mathbf{I}$, where $\frac{1}{\beta}$ denotes the variance of the PSF noise and $\mathbf{I}$ is the identity matrix. The observation vector $\mathbf{g}$ is also contaminated by zero-mean additive white noise with $N \times N$ covariance matrix $\mathbf{R}_{\Delta g} = \frac{1}{\gamma}\mathbf{I}$, where $\frac{1}{\gamma}$ denotes the variance of the observation noise. Furthermore, the noises in the observed data and the PSF are assumed independent of each other and independent from the source image $\mathbf{f}$. In this case, the image-degradation can be described by the model [2, 3, 4, 6]

$$\mathbf{g} = \mathbf{H}\mathbf{f} + \Delta\mathbf{g} \tag{3}$$

in which

$$\mathbf{H} = \bar{\mathbf{H}} + \Delta\mathbf{H}, \tag{4}$$

and $\mathbf{g}, \mathbf{f}, \Delta\mathbf{g} \in \mathcal{R}^N$ are lexicographically ordered representations of the observed degraded image, the source image, and the additive noise in the observed image, respectively. The matrix $\bar{\mathbf{H}}$ is the known (assumed, estimated or measured) component of the $N \times N$ PSF matrix $\mathbf{H}$; $\Delta\mathbf{H}$ is the unknown component of the PSF matrix, generated by $\Delta\mathbf{h}$ defined in (2).

From Eqs. (2)-(4) it is clear that the form of the conditional distribution of $\mathbf{g}$ is not simple. In what follows we propose two models for $P(\mathbf{g}|\mathbf{f}, \alpha, \beta, \gamma)$.

2.1.1 Fixed-f covariance model

For this model we use a Gaussian assumption for both the PSF noise $\Delta\mathbf{h}$ and the additive noise $\Delta\mathbf{g}$, see (2)-(4). Then, to determine $P(\mathbf{g}|\mathbf{f}, \alpha, \beta, \gamma)$ since vector $\mathbf{f}$ is not a random quantity but rather a fixed one, following [4], it is straightforward to see from (3) that $P(\mathbf{g}|\mathbf{f}, \alpha, \beta, \gamma)$ is given by

$$P(\mathbf{g}|\mathbf{f}, \alpha, \beta, \gamma) \propto \left[\det(\mathbf{R}_{g|f})\right]^{-\frac{1}{2}} \exp\left\{-\tfrac{1}{2}(\mathbf{g} - \bar{\mathbf{H}}\mathbf{f})^t \mathbf{R}_{g|f}^{-1}(\mathbf{g} - \bar{\mathbf{H}}\mathbf{f})\right\}. \tag{5}$$

The conditional covariance $\mathbf{R}_{g|f}$ in (5) is given by

$$\begin{aligned} \mathbf{R}_{g|f} &= E\left\{(\Delta\mathbf{H}\mathbf{f} + \Delta\mathbf{g})(\Delta\mathbf{H}\mathbf{f} + \Delta\mathbf{g})^t | \mathbf{f}\right\} \\ &= E\left\{(\mathbf{F}\Delta\mathbf{h} + \Delta\mathbf{g})(\mathbf{F}\Delta\mathbf{h} + \Delta\mathbf{g})^t | \mathbf{f}\right\}, = \\ &\quad E\left\{\Delta\mathbf{h}\Delta\mathbf{h}^t\right\}\mathbf{F}^t + E\left\{\Delta\mathbf{g}\Delta\mathbf{g}^t\right\} \\ &= \mathbf{F}\mathbf{R}_{\Delta h}\mathbf{F}^t + \mathbf{R}_{\Delta g} = \tfrac{1}{\beta}\mathbf{F}\mathbf{F}^t + \tfrac{1}{\gamma}\mathbf{I}, \end{aligned} \tag{6}$$

where we have used the commutative property of the convolution operation, $\mathbf{F}$ denotes the circulant matrix generated by the image $\mathbf{f}$, $\Delta\mathbf{h}$ is the unknown PSF noise vector from (2) and $E\{\ \}$ denotes the expectation operator.

2.1.2 Averaged-f covariance model

For this model we assume that the *observations* $\mathbf{g}$ are Gaussian and instead of using $\mathbf{F}\mathbf{F}^t$ in the expression for the covariance we use its mean value from the prior. In other words, the expectation in (6) is taken over $\mathbf{f}$ also. Thus, for this model we get

$$\underline{\mathbf{R}}_{g|f} = [\frac{N}{\beta}(\alpha\mathbf{Q}^t\mathbf{Q})^{-1} + \frac{\mathbf{I}}{\gamma}]^{-1}. \tag{7}$$

Note that by using this approximation we have incorporated the uncertainty of the image prior model, α, in the conditional distribution. Thus, the $\log P(\mathbf{g}|\mathbf{f}, \alpha, \beta, \gamma)$ is quadratic function with respect to $\mathbf{f}$. This yields a linear estimator for $\mathbf{f}$ as will be shown.

3 Hierarchical Bayesian Analysis

According to the evidence analysis (EA) framework [1] the simultaneous estimation of $\mathbf{f}$, α, β, and γ is done as follows:

Parameter estimation step:

$$\hat{\alpha}, \hat{\beta}, \hat{\gamma} = \arg\max_{\alpha,\beta,\gamma}\{P(\alpha, \beta, \gamma|\mathbf{g})\}. \tag{8}$$

Restoration step:

$$\hat{\mathbf{f}}(\hat{\alpha}, \hat{\beta}, \hat{\gamma}) = \arg\max_{\mathbf{f}}\left\{P(\mathbf{f}|\mathbf{g}, \hat{\alpha}, \hat{\beta}, \hat{\gamma})\right\}. \tag{9}$$

The estimates $\hat{\alpha}$, $\hat{\beta}$, and $\hat{\gamma}$ from the parameter estimation step depend on the current estimate of the image. Likewise, the estimate $\hat{\mathbf{f}}$ from the restoration step will depend on current estimates of the parameters. Therefore, the above two-step procedure is repeated until convergence occurs.

In order to find $P(\alpha, \beta, \gamma|\mathbf{g})$, as required by the parameter estimation step, we take into account that from the distributions defined in section 2 we have

$$\begin{aligned} &P(\mathbf{g}, \mathbf{f}, \alpha, \beta, \gamma) = \\ &P(\mathbf{g}|\mathbf{f}, \alpha, \beta, \gamma)P(\mathbf{f}|\alpha, \beta, \gamma)P(\alpha)P(\beta)P(\gamma). \end{aligned} \tag{10}$$

Then, to obtain $P(\alpha, \beta, \gamma|\mathbf{g})$ as required in (8) we marginalize the PDF in (10) with respect to $\mathbf{f}$ [1],[5], i.e.,

$$P(\alpha, \beta, \gamma|\mathbf{g}) \propto \int P(\mathbf{g}, \mathbf{f}, \alpha, \beta, \gamma)d\mathbf{f}. \tag{11}$$

Since we assumed "flat" non-informative hyperpriors, $P(\alpha)P(\beta)P(\gamma)$ can be discarded in (10) and so we have

$$P(\mathbf{g},\mathbf{f},\alpha,\beta,\gamma) \propto P(\mathbf{f}|\alpha,\beta,\gamma)P(\mathbf{g}|\mathbf{f},\alpha,\beta,\gamma). \quad (12)$$

The use of Gamma hyperpriors for this problem is described in [4].

Now, as required in (9) for the restoration step, the image *posterior* PDF $P(\mathbf{f}|\mathbf{g},\hat{\alpha},\hat{\beta},\hat{\gamma})$ can be obtained applying Bayes rule to the joint PDF, i.e.,

$$P(\mathbf{f}|\mathbf{g},\hat{\alpha},\hat{\beta},\hat{\gamma}) \propto P(\mathbf{f}|\hat{\alpha},\hat{\beta},\hat{\gamma})P(\mathbf{g}|\mathbf{f},\hat{\alpha},\hat{\beta},\hat{\gamma}), \quad (13)$$

where $P(\mathbf{f}|\hat{\alpha},\hat{\beta},\hat{\gamma})$ and $P(\mathbf{g}|\mathbf{f},\hat{\alpha},\hat{\beta},\hat{\gamma})$ are given in Eqs. (1) and (5) respectively, evaluated at $\hat{\alpha}$, $\hat{\beta}$, and $\hat{\gamma}$.

Using the two different choices for $P(\mathbf{g}|\mathbf{f},\alpha,\beta,\gamma)$ given in Eqs. (5) and (6) we proceed with the evidence analysis.

4 The Fixed-f Covariance Model

Substituting (1) and (5) into (10) we obtain

$$P(\mathbf{g},\mathbf{f},\alpha,\beta,\gamma) \propto \alpha^{(\frac{N}{2})}[\det(\mathbf{R}_{g|f})]^{-\frac{1}{2}} \exp\left\{-\tfrac{1}{2}J(\mathbf{f},\alpha,\beta,\gamma)\right\}, \quad (14)$$

where

$$J(\mathbf{f},\alpha,\beta,\gamma) = \alpha||\mathbf{Q}\mathbf{f}||^2 + (\mathbf{g}-\bar{\mathbf{H}}\mathbf{f})^t\mathbf{R}_{g|f}^{-1}(\mathbf{g}-\bar{\mathbf{H}}\mathbf{f}). \quad (15)$$

Parameter Estimation Step

To compute $P(\alpha,\beta,\gamma|\mathbf{g})$ as required by the parameter estimation step we substitute (14) into (11). This gives

$$P(\alpha,\beta,\gamma|\mathbf{g}) \propto \alpha^{(\frac{N}{2})}\int[\det(\mathbf{R}_{g|f})]^{-\frac{1}{2}} \exp\left\{-\tfrac{1}{2}J(\mathbf{f},\alpha,\beta,\gamma)\right\}d\mathbf{f}. \quad (16)$$

Now we are ready to perform the integration in (16). First, we expand $J(\mathbf{f},\alpha,\beta,\gamma)$ in Taylor series around a known $\mathbf{f}^{(n)}$, where (n) denotes the iteration index, i. e.,

$$J(\mathbf{f},\alpha,\beta,\gamma) \approx J(\mathbf{f}^{(n)},\alpha,\beta,\gamma) + (\mathbf{f}-\mathbf{f}^{(n)})^t\nabla J(\mathbf{f},\alpha,\beta,\gamma)|_{\mathbf{f}^{(n)}} + \tfrac{1}{2}(\mathbf{f}-\mathbf{f}^{(n)})^t\nabla^2 J(\mathbf{f},\alpha,\beta,\gamma)|_{\mathbf{f}^{(n)}}(\mathbf{f}-\mathbf{f}^{(n)}). \quad (17)$$

Next we observe that in (17)

$$\nabla J(\mathbf{f},\alpha,\beta,\gamma)|_{\mathbf{f}^{(n)}} = 0, \quad (18)$$

if $\mathbf{f}^{(n)}$ is chosen to be the minimizer of $J(\mathbf{f},\alpha,\beta,\gamma)$ in (15), and that the Hessian matrix can be approximated by

$$\nabla^2 J(\mathbf{f},\alpha,\beta,\gamma)|_{\mathbf{f}^{(n)}} \simeq \mathbf{G}^{(n)} = \alpha\mathbf{Q}^t\mathbf{Q} + \bar{\mathbf{H}}^t\mathbf{R}_{g|f^{(n)}}^{-1}\bar{\mathbf{H}}, \quad (19)$$

where we have not taken into account the derivatives of $\mathbf{R}_{g|f^{(n)}}^{-1}$ with respect to $\mathbf{f}$.

Finally, substituting (17) into (16), and by using the fact that $[\det\mathbf{R}_{g|f}]^{-\frac{1}{2}}$ depends on $\mathbf{f}$ weakly, compared to the exponential term under the integral and so it can be substituted by $[\det\mathbf{R}_{g|f^{(n)}}]^{-\frac{1}{2}}$ and that integral of a PDF is equal to 1, Eq. (16) becomes

$$P(\alpha,\beta,\gamma|\mathbf{g}) \propto \alpha^{(\frac{N}{2})}[\det\mathbf{R}_{g|f^{(n)}}]^{-\frac{1}{2}}[\det\mathbf{G}^{(n)}]^{-\frac{1}{2}} \exp\left\{-\tfrac{1}{2}J(\mathbf{f}^{(n)},\alpha,\beta,\gamma)\right\}. \quad (20)$$

It is interesting to note that the *posterior* functional in (20) is equivalent to the likelihood functional $P(\mathbf{g}|\mathbf{f},\alpha,\beta,\gamma)$ for this problem since we assumed uniform priors on α, β, and γ.

In the above equations we have used the fact that $[\det\mathbf{R}_{g|f}]^{-\frac{1}{2}}$ depends on $\mathbf{f}$ weakly, compared to the exponential term under the integral. To justify this we observe that the eigenvalues of $\mathbf{R}_{g|f}$ in (6) are given by

$$\frac{1}{\beta}|F(i)|^2 + \frac{1}{\gamma} = \frac{1}{\beta}NS_f(i) + \frac{1}{\gamma}, \quad (21)$$

where $F(i)$ is the i^{th} DFT coefficient of the image $\mathbf{f}$, and $S_f(i)$ is the periodogram estimate of the i^{th} power spectrum coefficient of the image $\mathbf{f}$ (the i^{th} eigenvalue of the image covariance matrix). The power spectrum (or the covariance matrix), however, is a statistic of $\mathbf{f}$; it depends on the class of images $\mathbf{f}$ belongs to, not on $\mathbf{f}$. The same reasons justify the approximation used for the Hessian.

Taking "2 log" of both sides of (20) we obtain the following functional:

$$L(\alpha,\beta,\gamma) = N\log\alpha - \log\det\mathbf{R}_{g|f^{(n)}} - \log\det\mathbf{G}^{(n)} - J(\mathbf{f}^{(n)},\alpha,\beta,\gamma), \quad (22)$$

which needs to be minimized.

To minimize this funtional we can use the following iterative scheme whose complete derivation can be found in [4]:

$$\frac{1}{\alpha^{(n+1)}} = \left[||\mathbf{Q}\,\mathbf{f}^{(n)}||^2 + \mathrm{tr}(\mathbf{G}^{(n)^{-1}}\mathbf{Q}^t\mathbf{Q})\right]/N, \quad (23)$$

$$\frac{1}{\beta^{(n+1)}} = \mathrm{tr}(\mathbf{R}_{g|f^{(n)}}^{-1})/N\beta^{(n)}\gamma^{(n)} + [\mathrm{tr}(\mathbf{G}^{(n)^{-1}}\bar{\mathbf{H}}^t\mathbf{R}_{g|f^{(n)}}^{-2}\mathbf{F}^{(n)}\mathbf{F}^{(n)^t}\bar{\mathbf{H}}) + (\mathbf{g}-\bar{\mathbf{H}}\mathbf{f}^{(n)})^t\mathbf{R}_{g|f^{(n)}}^{-2}\mathbf{F}^{(n)}\mathbf{F}^{(n)^t}(\mathbf{g}-\bar{\mathbf{H}}\mathbf{f}^{(n)})]/N\beta^{(n)^2}, \quad (24)$$

$$\frac{1}{\gamma^{(n+1)}} = \mathrm{tr}(\mathbf{F}^{(n)}\mathbf{F}^{(n)^t}\mathbf{R}_{g|f^{(n)}}^{-1})/N\beta^{(n)}\gamma^{(n)} + [\mathrm{tr}(\mathbf{G}^{(n)^{-1}}\bar{\mathbf{H}}^t\mathbf{R}_{g|f^{(n)}}^{-2}\bar{\mathbf{H}}) + (\mathbf{g}-\bar{\mathbf{H}}\mathbf{f}^{(n)})^t\mathbf{R}_{g|f^{(n)}}^{-2}(\mathbf{g}-\bar{\mathbf{H}}\mathbf{f}^{(n)})]/N\gamma^{(n)^2}, \quad (25)$$

where $\mathbf{f}^{(n)}$, $\mathbf{G}^{(n)}$, $\mathbf{F}^{(n)}$, $\alpha^{(n)}$, $\beta^{(n)}$, $\gamma^{(n)}$ are calculated at iteration (n). It is important to note that this iterative

scheme can also be carried out in the Fourier domain, (see [4]).

The parameter estimation cycle in (23)-(25) is repeated until convergence in (22) occurs. Although the proof of convergence of the resulting parameter estimators seems to be analytically intractable, in all our experiments with this EA algorithm we observed not only convergence in the *posterior* functional, but also in terms of the parameter values.

Restoration Step

To perform the restoration step we take into account that

$$\arg\min_{\mathbf{f}}\{P(\mathbf{f}|\mathbf{g},\alpha,\beta,\gamma)\} = \arg\min_{\mathbf{f}}\{P(\mathbf{f},\mathbf{g},\alpha,\beta,\gamma)\}. \tag{26}$$

As a result substituting (14) and (15) into (26) we get

$$\hat{\mathbf{f}}(\hat{\alpha},\hat{\beta},\hat{\gamma}) = \arg\min_{\mathbf{f}}\{(\bar{\mathbf{H}}\mathbf{f}-\mathbf{g})^t\hat{\mathbf{R}}_{g|f}^{-1}(\bar{\mathbf{H}}\mathbf{f}-\mathbf{g}) + \hat{\alpha}||\mathbf{Q}\,\mathbf{f}||^2 + \log[\det(\hat{\mathbf{R}}_{g|f})]\}, \tag{27}$$

where $\hat{\mathbf{R}}_{g|f} = \frac{1}{\hat{\beta}}\mathbf{F}\mathbf{F}^t + \frac{1}{\hat{\gamma}}$. The functional in (27) is non-convex and may have several local minima. In general, a closed form solution to (27) does not exist and numerical optimization algorithms must be used. A practical computation of (27) can be obtained by transforming it to the DFT domain. In [4] we show that minimization of (27) can be performed in the DFT domain as follows:

$$\hat{F}(i) = \arg\min_{F(i)} \frac{1}{N}\left[\frac{|\bar{H}(i)F(i)-G(i)|^2}{\frac{1}{\hat{\beta}}|F(i)|^2+\frac{1}{\hat{\gamma}}} + \hat{\alpha}|Q(i)|^2|F(i)|^2\right] + \log[\tfrac{1}{\hat{\beta}}|F(i)|^2 + \tfrac{1}{\hat{\gamma}}], \tag{28}$$

for each frequency $i = 0, 1, \cdots, N-1$. In (28) $G(i)$ and $F(i)$ are the DFT coefficients of the observed and restored images, $\bar{H}(i)$ and $Q(i)$ are the eigenvalues of $\bar{\mathbf{H}}$ and $\mathbf{Q}$, $\hat{\alpha}$, $\hat{\beta}$, and $\hat{\gamma}$ are the estimates of the hyperparameters obtained in the parameter estimation step and $|\cdot|$ denotes the modulus of a complex quantity. To implement the restoration step of the EA approach we minimized (28) with respect to the real and the imaginary parts of $F(i)$ for every discrete frequency i using the Davidon-Fletcher-Powell optimization algorithm. The gradient required by this algorithm was found in closed form.

The "log" term in (28) is weakly dependent on $\mathbf{f}$ and can be discarded when optimizing with respect to $\mathbf{f}$. We verified this experimentally by comparing the solutions of (28) with and without the "log" term. We used a number of choices for the initial points for our optimization algorithm (the source, the degraded, and the EM-restored images) to test the point of convergence. In all cases we found that the selection of the initial points did not alter the solution of (28), regardless of whether the "log" term was present. Thus, for all practical purposes in the restoration step we minimize $J(\mathbf{f},\alpha,\beta,\gamma)$ with respect to $\mathbf{f}$.

5 The Averaged-f Covariance Model

Using (5) as the likelihood equation we derive another iterative parameter estimation-image restoration algorithm for this problem. We follow identical steps as in the previous section with

$$\underline{\mathbf{R}}_{g|f} = \frac{N}{\beta}(\alpha\mathbf{Q}^t\mathbf{Q})^{-1} + \frac{\mathbf{I}}{\gamma}. \tag{29}$$

Taking "2 log" of the corresponding $P(\alpha,\beta,\gamma|\mathbf{g})$ yields a similar form to Eq. (22) log-likelihood function given by

$$\underline{L}(\alpha,\beta,\gamma) = N\log\alpha - \log\det\underline{\mathbf{R}}_{f|g} - \log\det\underline{\mathbf{G}} - \underline{J}(\mathbf{f}^{(n)},\alpha,\beta,\gamma), \tag{30}$$

where

$$\underline{J}(\mathbf{f}^{(n)},\alpha,\beta,\gamma) = \alpha||\mathbf{Q}\mathbf{f}^{(n)}||^2 + (\mathbf{g}-\bar{\mathbf{H}}\mathbf{f}^{(n)})^t\underline{\mathbf{R}}_{g|f}^{-1}(\mathbf{g}-\bar{\mathbf{H}}\mathbf{f}^{(n)}), \tag{31}$$

and

$$\nabla^2\tilde{J}(\mathbf{f},\alpha,\beta,\gamma)|_{\mathbf{f}^{(n)}} = \underline{\mathbf{G}} = \alpha\mathbf{Q}^t\mathbf{Q} + \bar{\mathbf{H}}^t\underline{\mathbf{R}}_{g|f}^{-1}\bar{\mathbf{H}}. \tag{32}$$

Clearly, the functional relationship of β and γ remains the same in the two likelihood functions $L(\alpha,\beta,\gamma)$ in (22) and $\underline{L}(\alpha,\beta,\gamma)$ in (30). However, the functional relationship of α changes in (22) and (30). Therefore, we expect the update equations for β and γ to be very similar to the ones of the previous algorithm but not the update for α. Furthermore, since $\underline{\mathbf{R}}_{f|g}$ does not depend on $\mathbf{f}$, $\underline{J}(\mathbf{f}^{(n)},\alpha,\beta,\gamma)$ is quadratic with respect to $\mathbf{f}$. As a result, the image restoration step gives a linear estimate for $\mathbf{f}$ for this algorithm.

Parameter Estimation Step

To find estimates of the parameters $\underline{L}(\alpha,\beta,\gamma)$ must be minimized. Taking the derivatives of $\underline{L}(\alpha,\beta,\gamma)$ with respect to α,β,γ gives identical parameter estimation equations to (24) and (25) if $\mathbf{F}^{(n)}\mathbf{F}^{(n)t}$ is replaced by $(\alpha\mathbf{Q}^t\mathbf{Q})^{-1}$. The above algorithm is identical to the EM-based algorithm derived for this problem in [3, 4].

Image Restoration Step

For the image estimation step, similar to (27), we can write

$$\hat{\mathbf{f}}(\hat{\alpha},\hat{\beta},\hat{\gamma}) = \arg\min_{\mathbf{f}}\left\{\underline{J}(\mathbf{f},\hat{\alpha},\hat{\beta},\hat{\gamma})\right\} = \arg\min_{\mathbf{f}}\{(\bar{\mathbf{H}}\mathbf{f}-\mathbf{g})^t\underline{\mathbf{R}}_{g|f}^{-1}(\bar{\mathbf{H}}\mathbf{f}-\mathbf{g}) + \hat{\alpha}||\mathbf{Q}\,\mathbf{f}||^2 + \log[\det(\underline{\mathbf{R}}_{g|f})]\}, \tag{33}$$

where $\underline{\mathbf{R}}_{g|f} = \frac{N}{\hat{\beta}}(\hat{\alpha}\mathbf{Q}^t\mathbf{Q})^{-1} + \frac{1}{\hat{\gamma}}\mathbf{I}$. This minimization yields a linear estimator

$$\hat{\mathbf{f}}(\hat{\alpha},\hat{\beta},\hat{\gamma}) = [\bar{\mathbf{H}}^t(\underline{\mathbf{R}}_{g|f})^{-1}\bar{\mathbf{H}} + \hat{\alpha}\mathbf{Q}^t\mathbf{Q}]^{-1}\bar{\mathbf{H}}^t(\underline{\mathbf{R}}_{g|f})^{-1}\mathbf{g}. \tag{34}$$

6 Experiments

We tested and compared the proposed EB algorithms. In what follows we shall refer to the one based on the *fixed*-$\mathbf{f}$ covariance model as EA1 and the other one which is identical to the EM as EA2. The (per pixel) MSE is defined as MSE $= \frac{1}{N}\|\mathbf{f} - \hat{\mathbf{f}}\|_2^2$, where $\mathbf{f}$ and $\hat{\mathbf{f}}$ are the original and the restored (upon convergence) images, respectively. The MSE measurements were performed based on Monte-Carlo simulations. To avoid plotting the 3-D plot of the MSE versus both noise parameters we plot two 2-D MSE plots: (Plot-H): For a fixed $\text{SNR}_g = 30dB$ we plot MSE versus SNR_h by varying $\frac{1}{\beta}$, and (Plot-G): For a fixed $\text{SNR}_h = 20dB$ we plot MSE versus SNR_g by varying $\frac{1}{\gamma}$. In those plots the noise parameters are expressed in terms of the signal-to-noise ratios (SNR), i.e., $\text{SNR}_h = \frac{\|\bar{\mathbf{h}}\|^2}{N\frac{1}{\beta}}$, $\text{SNR}_g = \frac{\|\mathbf{f}\|^2}{N\frac{1}{\gamma}}$, where $\|\bar{\mathbf{h}}\|^2$ and $\|\mathbf{f}\|^2$ are the energies of the known part of the PSF, and the original image, respectively. In all experiments presented in this paper Gaussian-shaped PSF given below was used for blurring: $h(i,j) = c \cdot \exp\left\{-\frac{i^2+j^2}{2\cdot 3^2}\right\}$, for $i,j = -15,\cdots,15$, where c is a constant chosen so that $\sum_{i,j} h(i,j) = 1$.

Experiment I. In this experiment we assume white-noise PSF perturbations with exact knowledge of the noise parameters $\frac{1}{\beta}$ and $\frac{1}{\gamma}$. The "Lena" image was used in this experiment. The parameter α was estimated by the algorithm. The MSEs of the EA1 and EA2 for fixed SNR_h and SNR_g are shown in Figures 1 and 2, respectively.

Experiment II. In this experiment EA1 and the EA2 algorithms are compared under the correlated PSF perturbations. More specifically, we assume that the PSFs used for blurring and restoration are Gaussian shaped, but with different widths. The blurring PSF had standard deviation 3.0 while the restoring PSF had standard deviation 4.0. The "Lena" image was used in this experiment. The spectrum of the PSF errors was assumed uknown and was modeled as white noise. In other words the algorithms estimated both parameter $\frac{1}{\gamma}$ and $\frac{1}{\alpha}$. The constant-$\frac{1}{\gamma}$ MSE plot for this experiment is given in Figure 3.

From the previous experiments we observed that the two algorithms give almost identical results when the PSF noise is white while EA2 is much faster. However, for colored noise EA1 outperforms EA2. This leads to the conclusion that for colored PSF noise the approximation used in EA2 is not accurate.

References

[1] Berger J. O., *Statistical Decision Theory and Bayesian Analysis,* Springer-Verlag, New York, 1985.

[2] Mesarović V. Z., Galatsanos N. P., and Katsaggelos A. K., "Regularized Constrained Total Least-Squares Image Restoration", *IEEE Trans. Image Processing*, Vol. 4, No. 8, pp. 1096-1108, August 1995.

[3] Mesarović V. Z., Galatsanos N. P., and Wernick M. N., "Restoration from Partially-Known Blur Using an Expectation-Maximization Algorithm", *Proceedings of Thirtieth ASILOMAR conference*, pp. 95-100, Pacific Grove, November 1996.

[4] Mesarović V. Z. , *Image Restoration Problems Under Point-Spread Function Uncertainties,* Ph. D. Thesis, ECE Dept., Illinois Institute of Technology, Chicago, May 1997.

[5] Molina R., "On the Hierarchical Bayesian Approach to Image Restoration: Applications to Astronomical Images", *IEEE Trans. on Pattern Analysis and Machine Inteligence,* Vol. 16, No. 11, pp. 1122-1128, November 1994.

[6] Ward R. K. and Saleh B. E. A., "Restoration of Images Distorted by Systems of Random Impulse Response", *Journal of the Optical Society of America A.,* Vol. 2, No.8, pp. 1254-1259, August 1985.

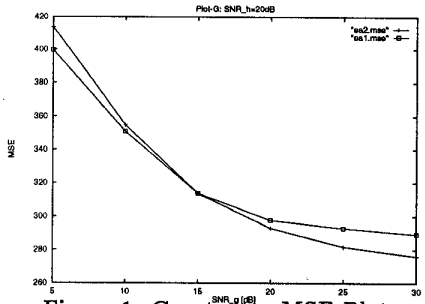

Figure 1. Constant-γ MSE Plot

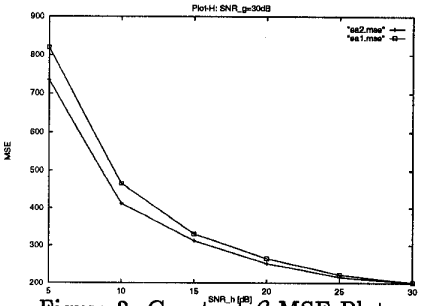

Figure 2. Constant-β MSE Plot

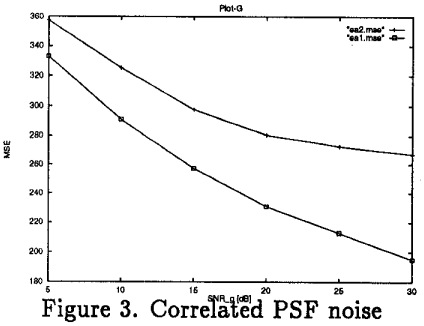

Figure 3. Correlated PSF noise